Hindawi
Journal of Nanotechnology
Volume 2022, Article ID 7406168, 9 pages
https://doi.org/10.1155/2022/7406168

Research Article

Optimization of Antibacterial, Structures, and Thermal Properties of Alginate-ZrO_2 Bionanocomposite by the Taguchi Method

Mohsen Safaei,[1,2] **Hedaiat Moradpoor**,[3] **Mohammad Salmani Mobarakeh**,[4] **and Nima Fallahnia**[2,5]

[1]*Division of Dental Biomaterials, School of Dentistry, Kermanshah University of Medical Sciences, Kermanshah, Iran*
[2]*Advanced Dental Sciences Research Center, School of Dentistry, Kermanshah University of Medical Sciences, Kermanshah, Iran*
[3]*Department of Prosthodontics, School of Dentistry, Kermanshah University of Medical Sciences, Kermanshah, Iran*
[4]*Department of Materials Engineering, Isfahan University of Technology, Isfahan 84156-83111, Iran*
[5]*Student Research Committee, Kermanshah University of Medical Sciences, Kermanshah, Iran*

Correspondence should be addressed to Nima Fallahnia; fallahnianima@gmail.com

Received 7 August 2022; Revised 22 November 2022; Accepted 5 December 2022; Published 13 December 2022

Academic Editor: Amit Mandal

Developing novel antibacterial chemicals is constantly necessary since bacterial resistance to antibiotics is an inevitable occurrence. This research aimed to find the ideal conditions for using antibacterial zirconia (ZrO_2) NPs with polymer alginate nanocomposites. Using the Taguchi method, alginate biopolymer, zirconia NPs, and stirring time were utilized to construct nine nanocomposites. Analysis of Fourier transform infrared spectroscopy (FTIR), ultraviolet-visible (UV-vis), spectroscopy, X-ray diffraction (XRD), scanning electron microscopy (SEM), energy-dispersive X-ray spectroscopy (EDX), transmission electron microscopy (TEM), and thermogravimetric analysis (TGA) indicated the development of nanocomposites with appropriate structural properties. Antibacterial efficacy against *Streptococcus mutans* (*S. mutans*) biofilm was the highest when the nanocomposite was formed under the circumstances of experiment 6 (zirconia 8 mg/ml, alginate 70 mg/ml, and 40 min stirring time). Alginate/zirconia bionanocomposites generated using the in situ technique proved efficient against *S. mutans*. Nanoparticles have a high surface-to-volume ratio and surface energy, which can cause them to agglomerate and make their antimicrobial effectiveness problematic. Using zirconia nanoparticles in an alginate polymer matrix in the form of nanocomposite can increase the stability of nanoparticles. Due to the advantageous antibacterial qualities of this bionanocomposite, it can be utilized in various medical materials and dental appliances.

1. Introduction

Despite improving treatment methods in recent years, treating some diseases, such as cancer, AIDS, autoimmune disease, and antimicrobial resistance, is still a global challenge [1–3]. The emergence of antibiotic resistance has become one of the significant challenges due to the waste of large numbers of humans and economic losses [4]. Bacteria can form biofilms, but they pose additional challenges for antibiotic treatment [5]. *S. mutans* is a facultative anaerobic bacterium routinely found in dental plaque and can form biofilms by various mechanisms [6]. This bacterium can lead to dental caries, other cariogenic factors, pyogenic infections, and extraoral infections such as bacteremia and endocarditis [7, 8].

There are many alternative methods to deal with the problems of routine antibiotic therapies against bacteria biofilm forming, including *S. mutans*, each of which has its

challenges [5, 9]. One of the successful alternatives to routine antibiotics and counteracting the spread of antibiotic resistance is nanotechnology and the synthesis of nanoparticles (NPs) and nanocomposites with antimicrobial properties [10, 11]. Many applications of nanostructures are due to their physical properties, i.e., optical properties, small size, surface properties, and specific shape [12, 13]. Metal oxide NPs show much better antimicrobial activity than their bulky mass. In addition, it has been demonstrated that synthesizing nanocomposites containing natural polymers and incorporating metal NPs with them can enhance the biological activity of NPs [10, 11, 14].

Metal oxide NPs have been studied as one of the antimicrobial factors agents due to their optimal biocompatibility, including ZnO, TiO_2, MgO, CuO, and ZrO_2 NPs. Meanwhile, the antimicrobial properties of zirconia NPs have been less studied despite their mechanical properties and optimal biocompatibility [15, 16]. Zirconia can be a good candidate for many biomedical activities due to its strength, toughness, stability, relatively reasonable price, and biomimetic [17]. However, previous studies have shown that the synthesis of ZrO_2 NPs poses challenges due to agglomeration and poor crystallinity. In addition to these undesirable physical properties, it also exhibits minor biomedical activity [18, 19]. However, using ZrO_2 in polymeric nanocomposites has shown good antibacterial and antifungal properties and excellent physical properties such as good temperature resistance [17].

Alginate is a natural linear polysaccharide typically extracted from seaweed and can be produced by some bacterial species [20]. This biopolymer has found wide applications in medicine due to its properties, such as nontoxicity, biodegradability, biocompatibility, and most importantly, its unique chemical structure [21]. Alginate is constituted of variable amounts of β-D-mannuronic (M) and α-L-guluronic (G), which are organized in an irregular pattern by β-1,4-glycosidic bonds [21, 22]. The ratio of G and M blocks in the alginate structure and the resulting different conformations can affect this biopolymer's physical and biological properties [22]. Alginate can be used as a matrix in the synthesis of many nanocomposites. The presence of hydroxyl groups in the alginate structure allows it to interact with metal oxide NPs, which can improve its biological performance.

This research aimed to determine the ideal conditions for the synthesis of alginate/zirconia bionanocomposite as a novel antibacterial agent against *S. mutans* biofilm because the synthesis and antimicrobial activity of this bionanocomposite have not been assessed.

2. Materials and Methods

2.1. Synthesis of Zirconia Nanoparticles. Using the biosynthesis process, Halomonas elongata synthesized zirconia NPs. For this purpose, 100 ml of bacterial culture medium containing 0.2 g glucose, 3 g NaCl, 0.046 g NH_4Cl, 0.028 g $MgSO_4$, 0.011 g K_2HPO_4, and 0.0001 g of $FeSO_4$ was prepared and inoculated with *Halomonas elongata*. After incubating bacterial cells at 37°C for 48 h, they were centrifuged at 5000 for 15 min. The precipitate and supernatant were then separated, and the resulting supernatant was used to synthesize nanoparticles. Then, 0.5 ml of bacterial culture supernatant was added to 1 mg/ml of zirconium chloride. In a shaking incubator, the mixture was incubated for 72 h at 120 rpm, 32°C, and 1 mg/ml zirconium chloride concentration. Final solutions containing NPs were filtered with Whatman filter paper to remove contaminants and then sterilized with a microbial filter to ensure sterility. The product was put in an oven at 100°C for 24 h to obtain zirconia NPs powder.

2.2. Synthesis and Preparation of Alginate Biopolymer. The biosynthesis method produced an alginate biopolymer from the *Azotobacter Vinelandi* bacterium. This type of bacterium, IBRC-M 10786, was obtained from the Iranian center for biological resources for this purpose. The bacterium was then added to a culture medium and incubated for 72 h at 29°C with 150 rpm in a shaking incubator [23]. Centrifugation carried out at 5000 rpm for 10 min was 100 ml of the final culture medium containing 10 ml of 0.1 M ethylenediaminetetraacetic acid (EDTA) and 10 ml of 1 M sodium chloride [19]. The bacterial cells in the supernatant were precipitated, separated, transferred to a container containing isopropanol, and stirred with a magnetic stirrer for 20 min. To prepare an alginate biopolymer, a precipitate was collected, separated, and then dried in an oven at 40°C for 72 h using filter paper.

2.3. Synthesis of Alginate/Zirconia Bionanocomposite. Nine experiments were planned using Qulitek-4 software and the Taguchi method to assess antibacterial activity and establish the best situations for synthesizing nanocomposites with strong antibacterial characteristics [14]. Using the Taguchi method, three levels of 60, 70, and 80 mg/ml of alginate biopolymer and three levels of 4, 6, and 8 mg/ml of zirconia NPs were used to synthesize alginate/zirconia bionanocomposites at stirring times of 40, 80, and 120 min. For synthesizing the nine studied nanocomposites, zirconia NPs and alginate biopolymer were separately dissolved in solutions with concentrations determined using the Taguchi method. Each was sonicated for 15 min to create a homogeneous solution after being stirred for 60 min. Drop by drop, the zirconia NPs solution was added to the alginate biopolymer solution in the container with the help of a magnetic stirrer. At 25°C, a magnetic stirrer was used to stir the final solutions for 40, 80, and 120 min before the sonication process, for 15 min, to produce nanocomposites with varying biopolymer to nanoparticle ratios. The nanocomposites' powder was made by putting these solutions in an oven at 60°C.

2.4. Antibacterial Activity. This bacterium *S. mutans* (ATCC 35668) was procured from the Iranian Research Organization for Science and Technology (IROST) to analyze the antibacterial effectiveness of synthesized alginate/zirconia bionanocomposites. One day was spent cultivating

Table 1: Taguchi design of experiments and effects of alginate/zirconia-synthesized nanocomposites on the survival rate of *Streptococcus mutans*.

Experiment	Alginate (mg/ml)			ZrO_2 (mg/ml)			Stirring time (min)			Bacterial survival (CFU/ml)
	60	70	80	4	6	8	40	80	120	
1		60			4			40		4.11
2		60			6			80		1.89
3		60			8			120		1.22
4		70			4			80		2.83
5		70			6			120		1.39
6		70			8			40		0.87
7		80			4			120		3.27
8		80			6			40		1.96
9		80			8			80		1.06

S. mutans on brain heart infusion (BHI) agar to produce a single colony. The next step was to prepare a bacterial suspension at a concentration of 0.5 McFarland. For 72 h, the bacterial suspension was incubated at 37°C with a 96-well culture plate to form a biofilm. Refreshed BHI replaced the daily culture medium containing 2% sucrose and 1% mannose. After creating a biofilm, the surface was washed three times with phosphate-buffered saline (PBS) to eliminate planktonic *S. mutans*.

An incubation period of 24 hours was used to synthesize nanocomposite materials in each well. Biofilm viability was determined by isolating cells from well walls and incubating them at 37°C for 24 h. After three washes, the remaining cells adhering to the excellent wall were suspended in 1 ml of PBS buffer. The resultant suspension was then homogenized for two min using a vortex. The bacterial suspension was prepared by diluting ten times for the colony forming unit (CFU) test, then cultured on BHI agar plates and incubated at 37°C for 24 h. The number of colonies was then counted, and their mean was calculated. All experiments had three replications [24, 25].

2.5. Characterization. Various characterization methods were used to figure out the characteristics of synthesized nanocomposites and their constituents. Fourier transform spectroscopy (FTIR) (Thermo Company at RT/USA), X-ray diffraction (XRD) (Philips X 'Pert (40 kV, 30 mA)/Nederland), scanning electron microscopy (SEM) (TESCAN Company), MIRA (III model/Czech Republic), transmission electron microscopy (TEM) (TEM Philips EM208S/Nederland), ultraviolet-visible (UV-vis) spectroscopy (Shimadzu Company, UV-160 A model/Japan), and thermogravimetric analysis/differential scanning calorimeter (TGA-DTA) (TA Company, Q600 model) were used.

3. Results and Discussion

3.1. Antibacterial Activity. The alginate/zirconia bionanocomposites exhibiting the greatest antimicrobial properties were synthesized using the Taguchi method, which consists of nine experiments. The viability of *S. mutans* was studied concerning nanocomposites synthesized under various conditions (Table 1). Experiment 6 revealed that the synthesized nanocomposite exhibited the highest antibacterial activity against *S. mutans* at 70 mg/ml of alginate biopolymer, 8 mg/ml of zirconia NPs, and 40 min of stirring. In its presence, the bacterial viability reached the lowest value, 0.87 CFU/ml.

Table 2: The main effects of different levels of alginate, ZrO_2, and the stirring time on the survival rate of *Streptococcus mutans*.

Factors	Level 1	Level 2	Level 3
Alginate	2.41	1.70	2.10
ZrO_2	3.40	1.75	1.05
Stirring time	2.31	1.93	1.96

Biopolymer alginate/zirconia NPs and stirring time all impact the viability of *S. mutans*, according to Table 2. The outcomes showed that the stirring time at level 2, the biopolymer alginate factor at level 2, and the zirconia NPs factor at level 3 had the most significant effects on the viability of *S. mutans*. The interaction of factors that affect the viability of *S. mutans* is depicted in Table 3. The interaction between alginate biopolymer in the second level and stirring time in the first level had the most significant effect on the viability rate of *S. mutans* at 64.50%. The interaction between zirconia NPs at the third level and stirring time at the first level significantly affected the viability of *S. mutans* by 18.67%. Alginate biopolymer had the least interaction intensity index in the second level, while zirconia NPs had the highest at 12.03%.

Table 4 shows the variance analysis of the parameters affecting the viability of *S. mutans*. The zirconia NPs had the highest impact on the viability rate of *S. mutans* (88.19%), followed by alginate biopolymer (7.05%) and stirring time (2.08%). The ideal conditions for synthesizing alginate/zirconia bionanocomposites with the greatest antimicrobial activity were identified following comprehensive information evaluation and analysis of the effects and interactions of each factor (Table 5). Accordingly, zirconia NPs had the highest level, and stirring time exhibited a minor level of influence on the viability rate of *S. mutans*. At the same time, alginate biopolymer acted as a mediator between these two variables. The second level was optimal for alginate biopolymer and stirring time factors, while the third level was optimal for zirconia nanoparticles. *S. mutans* viability was estimated to be reduced to 0.54 CFU/ml, which is the closest value to the results of experiment 6 and almost better, according to the results. Previous studies reported that zirconia NPs do not show good antimicrobial activity against Gram-positive bacteria, especially *S. mutans* [17, 26]. This could be due to the surface charges of these nanoparticles, which do not allow proper interaction with the bacterial cell walls of *S. mutans* [15]. However, synthesizing polymer-based nanocomposites with zirconia NPs can enhance the antibacterial properties of these NPs against Gram-positive bacteria, which accords with the findings of the current research [27]. The antibacterial activity of NPs depends on their size at the nanoscale, shape, and high surface energy level [28]. Although the antibacterial mechanisms of zirconia NPs are not fully understood, this property appears to be due to the ability to destroy cell

Table 3: The interaction effects of studied factors on the survival rate of *Streptococcus mutans*.

Interacting factor pairs	Column	Severity index (%)	Optimum conditions
Alginate × stirring time	1 × 3	64.50	[2, 1]
ZrO_2 × stirring time	2 × 3	18.67	[3, 1]
Alginate × ZrO_2	1 × 2	12.03	[2, 3]

Table 4: The analysis of variance of factors affecting the survival rate of *Streptococcus mutans*.

Factors	DOF	Sum of squares	Variance	*F*-ratio (*F*)	Pure sum	Percent (%)
Alginate	2	0.76	0.38	11.72	0.70	7.05
ZrO_2	2	8.77	4.38	135.17	8.70	88.19
Stirring time	2	0.28	0.14	4.25	0.21	2.13

DOF, degree of freedom.

Table 5: The optimum conditions for the synthesis of alginate/zirconia nanocomposites with the highest antibacterial activity.

Factors	Level	Contribution
Alginate	2	0.37
ZrO_2	3	1.02
Stirring time	2	0.14
Total contribution from all factors		1.53
Current grand average of performance		2.07
Bacterial survival at optimum condition		0.54

membranes as well as increased reactive oxygen species (ROS), which interferes with mesosome function, prevents DNA replication and cell division, and results in bacterial death [29].

3.2. FTIR Analysis. Figure 1 depicts the FTIR spectra of alginate biopolymer (diagram (a)), zirconia NPs (diagram (b)), and synthesized nanocomposites (diagram (c)) in the 400–4000 cm^{-1} range of wavelength. The hydroxyl groups' tensile fluctuations were observed in the spectrum of alginate with a wide peak at 3415 cm^{-1}. The bands observed between 2920 and 1615 cm^{-1} were caused by C-H bond tension in the pyranoid ring and fluctuations in the carboxyl group. Additionally, the C-O bond tension was found to be associated with the peaks at 1290, 1100, and 940 cm^{-1}. The bands observed between 885 and 770 cm^{-1} were of low intensity due to the C-C tensile bond and the internal rotation of the C-O bond, respectively [22, 30].

The FTIR spectrum of zirconia NPs showed a peak related to OH bond tension at position 3417 cm^{-1} and a peak associated with OH bond bending at position 1651 cm^{-1}. Also confirming the existence of a Zr-O bond, the peak was observed at 503 cm^{-1} [31]. The observed peaks in the final spectrum of the nanocomposite were a combination of the peaks observed in the spectrum components. Alginate biopolymer and zirconia NPs form the final nanocomposite, indicating strong interactions between these two materials [32].

3.3. XRD Analysis. XRD analysis investigated the crystal structure of alginate biopolymer samples, zirconia NPs, and

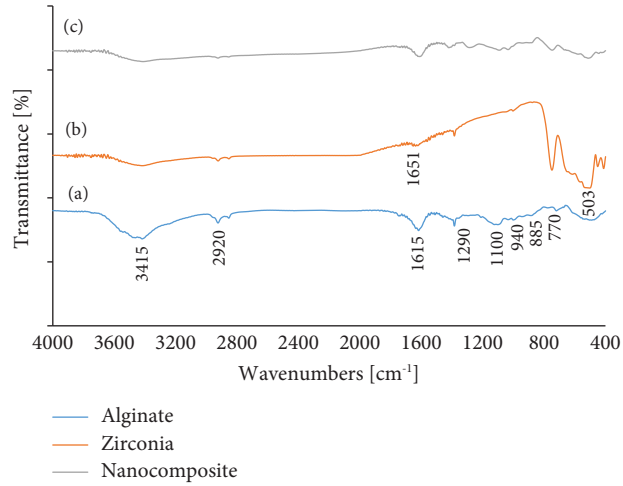

Figure 1: Fourier transform infrared spectroscopy (FTIR) spectra of the alginate biopolymer (a), zirconia NPs (b), and alginate/zirconia nanocomposites (c).

alginate/zirconia bionanocomposites (Figure 2). The alginate biopolymer (a) XRD spectrum showed an amorphous structure for this material. The XRD spectrum shows the synthesis of ZrO_2 NPs (b). The dispersed peaks in the diffraction pattern of zirconia NPs at angles 2θ (°) were observed respectively at 28.52 for the plane (–111), 31.72 for the plane (111), 34.46 for the plane (120), 50.54 for the plane (022), and 60.38 for the plane (131) and confirmed the formation of ZrO_2 with a monoclinic crystal structure [33]. The average crystal size was calculated to be 27 nm using the Scherrer equation for zirconia NPs. XRD spectra prepared from alginate/zirconia bionanocomposites (c) showed that the final structure was affected by NPs and alginate biopolymer, and the decrease in the intensity of the synthesized nanocomposite spectrum compared to the zirconia NPs confirmed the nanocomposite formation.

3.4. SEM Analysis. In Figure 3, the morphology of the alginate biopolymer (Figure 3(a)), zirconia NPs (Figure 3(b)), and prepared nanocomposite (Figure 3(c)) by field emission scanning electron microscopy were examined. The alginate biopolymer's SEM image showed this polymer's

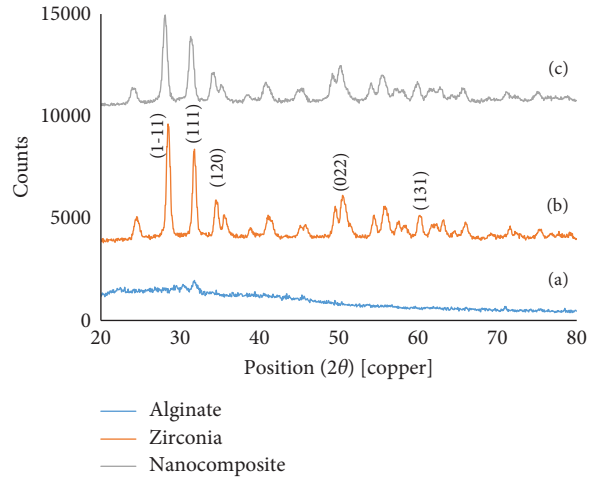

Figure 2: X-ray diffraction (XRD) patterns of alginate biopolymers (a), zirconia NPs (b), and alginate/zirconia nanocomposites (c).

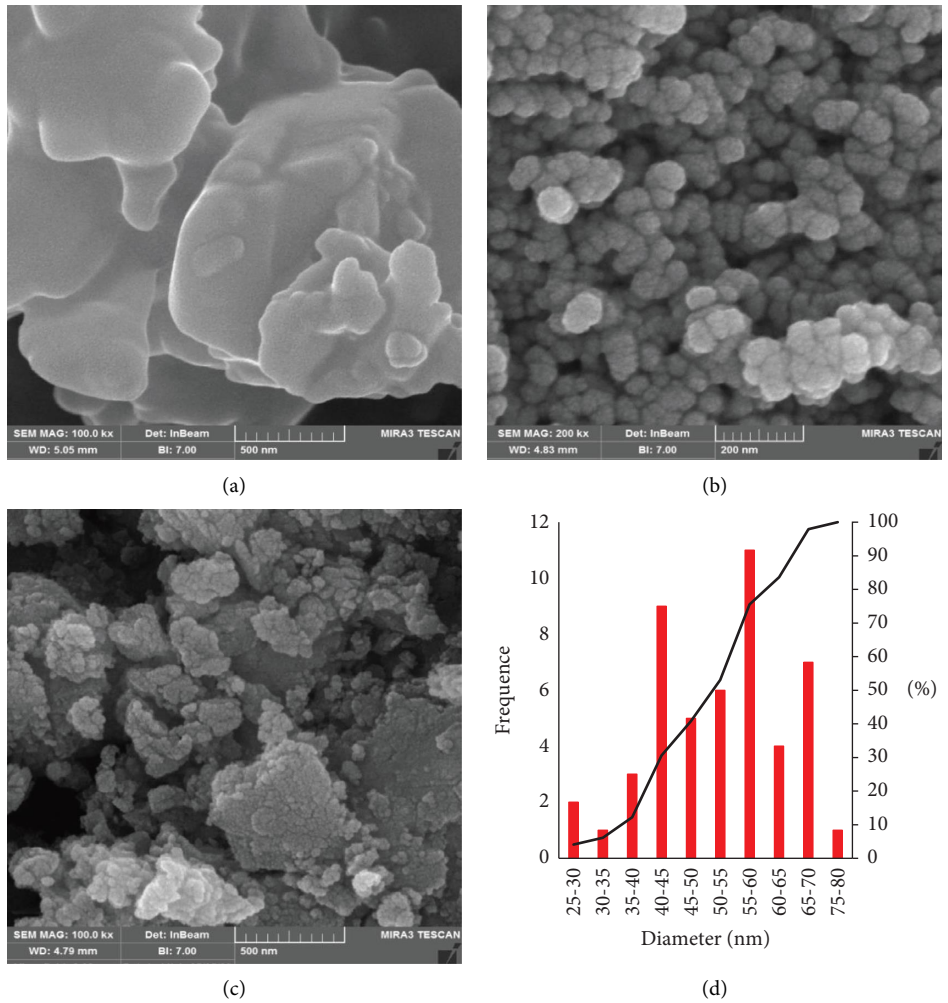

Figure 3: Scanning electron microscopy images of alginate biopolymers (a), zirconia NPs (b), alginate/zirconia nanocomposites (c), and the histogram of particle size distribution curves of zirconia NPs (d).

interconnected network. Sscanning electron microscopy of zirconia NPs showed agglomeration of some of these NPs and cluster shapes due to their high surface-to-volume ratio. The analysis of these images also revealed that the synthetic zirconium oxide NPs have an almost spherical shape. According to the SEM image, the approximate size range of

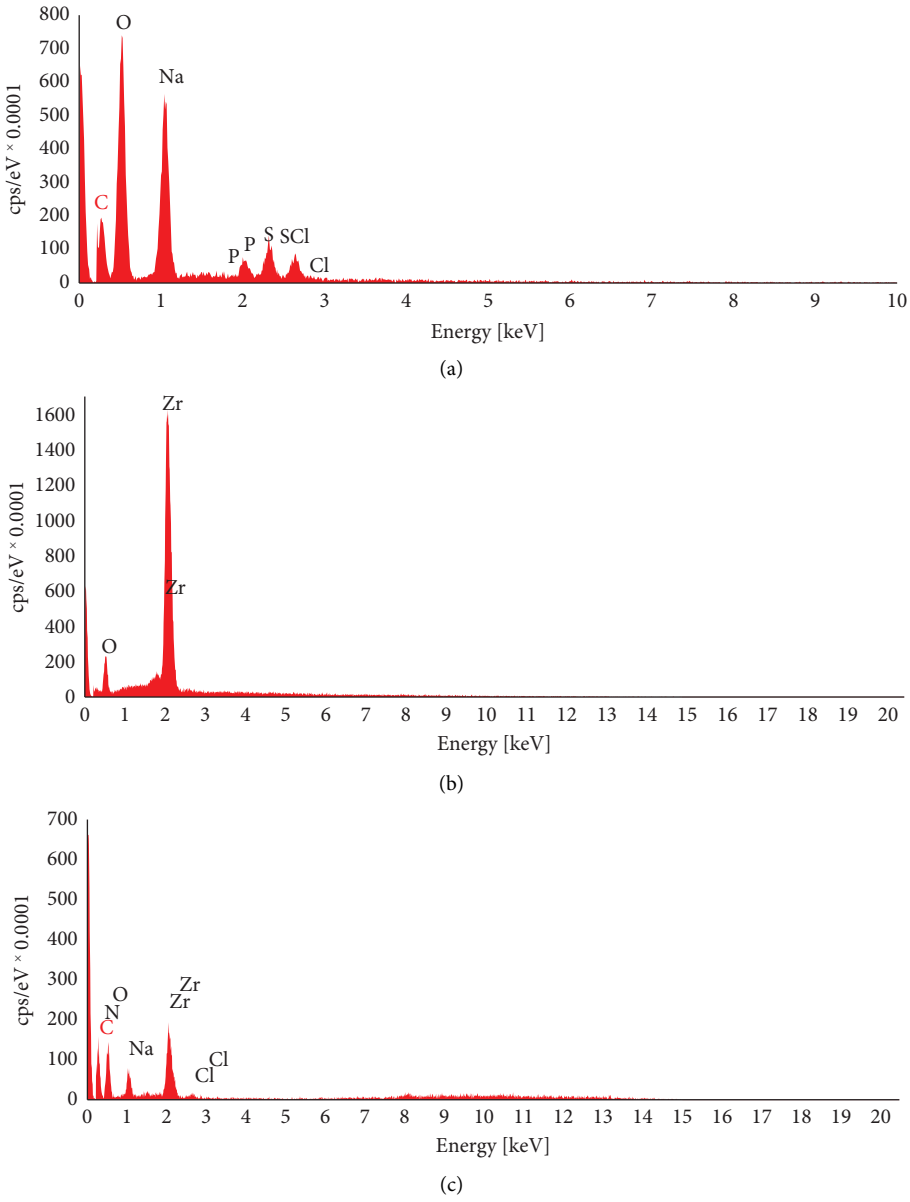

Figure 4: Energy-dispersive X-ray (EDX) spectra of alginate biopolymers (a), zirconia NPs (b), and alginate/zirconia nanocomposites (c).

the synthesized zirconia NPs ranges between 20 and 80 nm. Figure 3(d) depicts the histogram of the size distribution of these NPs and the maximum frequency corresponding to the size range from 55 to 60 nm. Nanocomposite networks were synthesized and coated with zirconia NPs as reinforcement for the alginate biopolymer, which could be seen in images of both the biopolymer and the synthesized nanocomposite.

3.5. EDX Analysis. Alginate biopolymer, zirconia nanoparticles, and alginate/zirconia bionanocomposites all had different constituent elements, according to energy-dispersive X-ray (EDX) results (Figure 4). These elements in the polymer alginate include oxygen, sodium, carbon, sulfur, phosphorus, and chlorine, with the highest peak intensity and the highest weight percentage, respectively

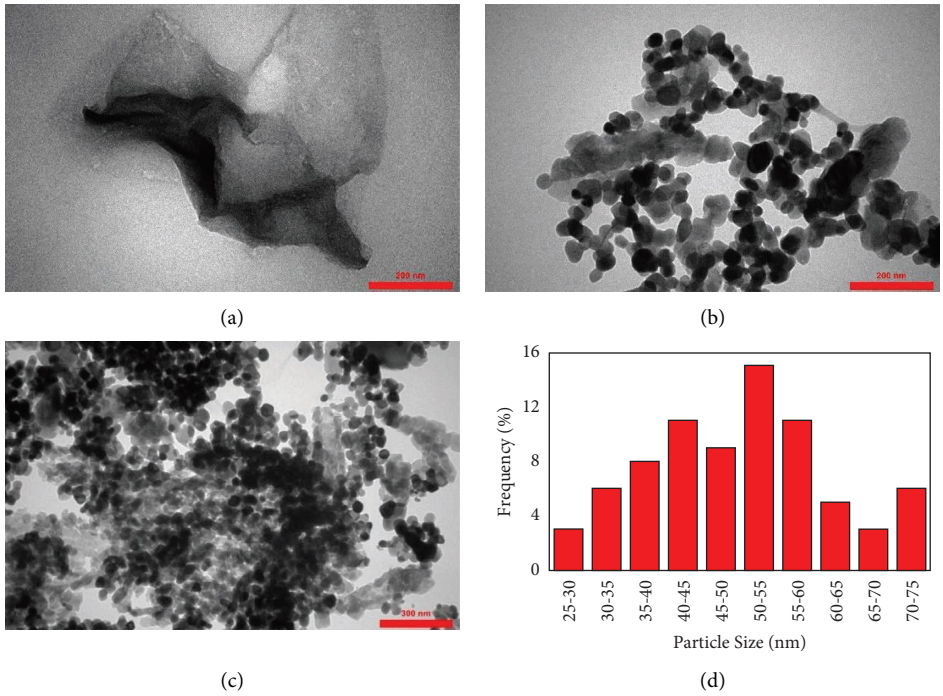

Figure 5: Transmission electron microscopy (TEM) images of alginate biopolymers (a), zirconia NPs (b), alginate/zirconia nanocomposites (c), and the histogram of particle size distribution curves of zirconia NPs (d).

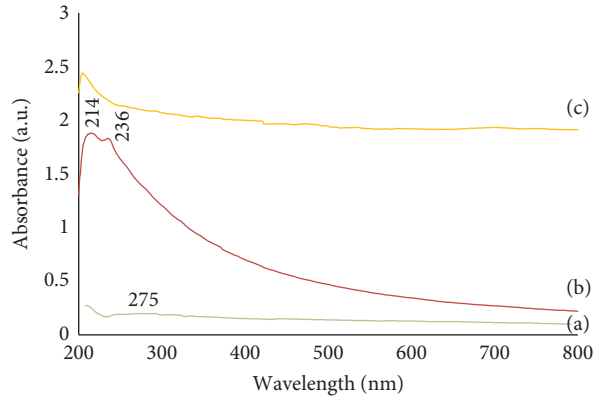

Figure 6: UV-vis spectroscopy analysis of the alginate biopolymer (a), zirconia NPs (b), and alginate/zirconia nanocomposites (c).

(Figure 4(a)). The EDX spectrum of zirconia NPs (Figure 4(b)) showed the presence of a high percentage of zirconium and an oxygen element, which confirmed the main constituents. The EDX graph prepared from alginate/zirconia bionanocomposites (Figure 4(c)) showed the presence of its constituent elements, which verified the synthesis of the nanocomposite.

3.6. TEM Analysis. Figure 5 displays the TEM micrograph prepared from the alginate polymer (Figure 5(a)), zirconia NPs (Figure 5(b)), and synthesized nanocomposites (Figure 5(c)). The morphology and particle size distribution of zirconia were also carefully examined by transmission electron microscopy. The shape of zirconia NPs was spherical. Also, the histogram of the size distribution of NPs showed that the maximum frequency was related to the size range from 50 to 55 nm (Figure 5(d)). TEM micrograph analysis confirmed the formation of alginate/zirconia bionanocomposites. The results demonstrated that the metal oxide NPs were dispersed in a biopolymer alginate matrix in a favorable manner and in various sizes.

3.7. UV-Vis Analysis. UV-vis spectroscopy investigated the optical properties of alginate/zirconia bionanocomposites and their constituents between 200 and 800 nm (Figure 6). Figure 6(a) shows an absorption band at 275 nm in the alginate biopolymer spectrum. Figure 6(b) also displays the UV-vis absorption spectrum for synthesizing zirconia NPs

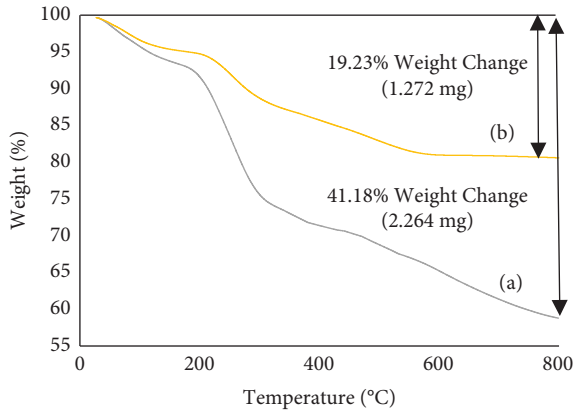

Figure 7: Thermogravimetric analysis of alginate biopolymers (a) and alginate-zirconia bionanocomposites (b).

in the 200–800 nm scan range. In the spectrum of zirconia NPs, two peaks were detected between 214 and 236 nm. The absorption spectra of the final synthesized nanocomposite (Figure 6(c)) demonstrate that the spectrum of the final nanocomposite is a combination of the properties of its constituents and that the final nanocomposite has been formed [30].

3.8. Thermal Analysis. Figure 7 presents the results of the thermal properties of the synthesized nanocomposite and alginate biopolymer. The thermogravimetric analysis curve of alginate biopolymer revealed four temperature ranges at which a certain percentage of mass was lost. Temperatures between 25 and 210°C resulted in an 8 percent weight loss, while temperatures between 312 and 475°C resulted in a 5.18 percent weight loss, and temperatures between 475°C and 800°C yielded an 11 percent weight loss (Figure 7(a)). The thermogravimetric diagram showed that the final synthesized nanocomposite has higher thermal stability than alginate biopolymer due to zirconia oxide NPs with high thermal stability in the synthesized nanocomposite (Figure 7(b)). Adding NPs to the polymer matrix altered the thermal stability of the nanocomposite, as manifested by a comparison of the thermogravimetric analysis curves for alginate polymer and nanocomposite samples.

4. Conclusions

Despite the variety of conventional antimicrobial agents, nanoparticles have a particular advantage because nanoparticles have a high surface-to-volume ratio. Therefore, it shows improved properties at their minimum concentration, and using nanoparticles as composite components can improve their stability and effectiveness. In this study, an alginate/zirconia bionanocomposite was tested for its antimicrobial property using the Taguchi method. The results showed that the in situ-produced nanocomposite was effective against *S. mutans* biofilm. Based on the antibacterial activity findings, it was estimated that under optimal conditions, nanocomposites could be synthesized (alginate 70 mg/ml, zirconia of 8 mg/ml, and stirring time of 80 min), and they significantly inhibited the formation of bacterial biofilm. In addition, various characterization methods confirmed that the investigated nanocomposite and its components had optimal structural properties. Due to its desirable antibacterial activity, this nanocomposite can be applied to various compounds in various fields. As an effective antibacterial agent, it can be a suitable alternative to the usual antibacterial agents with harmful effects.

Data Availability

The data used to support the findings of this study are included within the article.

Conflicts of Interest

The authors declare that they have no conflicts of interest.

Acknowledgments

The authors gratefully acknowledge the Research Council of Kermanshah University of Medical Sciences (Grant no. 980647) for the financial support.

References

[1] H. R. Mozaffari, B. Izadi, M. Sadeghi, F. Rezaei, R. Sharifi, and F. Jalilian, "Prevalence of oral and pharyngeal cancers in Kermanshah province, Iran: a ten-year period," *International Journal of Cancer Research*, vol. 12, no. 3-4, pp. 169–175, 2016.

[2] H. R. Mozaffari, E. Zavattaro, A. Abdolahnejad et al., "Serum and salivary IgA, IgG, and IgM levels in oral lichen planus: a systematic review and meta-analysis of case-control studies," *Medicina*, vol. 54, no. 6, p. 99, 2018.

[3] L. S. J. Roope, R. D. Smith, K. B. Pouwels et al., "The challenge of antimicrobial resistance: what economics can contribute," *Science*, vol. 364, no. 6435, p. 4679, 2019.

[4] N. E. Eleraky, A. Allam, S. B. Hassan, and M. M. Omar, "Nanomedicine fight against antibacterial resistance: an overview of the recent pharmaceutical innovations," *Pharmaceutics*, vol. 12, no. 2, p. 142, 2020.

[5] O. Ciofu, E. Rojo-Molinero, M. D. Macià, and A. Oliver, "Antibiotic treatment of biofilm infections," *Acta Pathologica, Microbiologica et Immunologica Scandinavica*, vol. 125, no. 4, pp. 304–319, 2017.

[6] Y. Cao, H. Yin, W. Wang et al., "Killing Streptococcus mutans in mature biofilm with a combination of antimicrobial and antibiofilm peptides," *Amino Acids*, vol. 52, no. 1, pp. 1–14, 2020.

[7] S. D. Forssten, M. Björklund, and A. C. Ouwehand, "Streptococcus mutans, caries and simulation models," *Nutrients*, vol. 2, no. 3, pp. 290–298, 2010.

[8] M. Nilsson, T. H. Jakobsen, M. Givskov, S. Twetman, and T. Tolker-Nielsen, "Oxidative stress response plays a role in antibiotic tolerance of Streptococcus mutans biofilms," *Microbiology*, vol. 165, no. 3, pp. 334–342, 2019.

[9] T. Cui, W. Luo, L. Xu, B. Yang, W. Zhao, and H. Cang, "Progress of antimicrobial discovery against the major cariogenic pathogen Streptococcus mutans," *Current Issues In Molecular Biology*, vol. 32, pp. 601–644, 2019.

[10] M. Safaei and M. Taran, "Optimal conditions for producing bactericidal sodium hyaluronate-TiO_2 bionanocomposite and

its characterization," *International Journal of Biological Macromolecules*, vol. 104, pp. 449–456, 2017.

[11] M. Taran, S. Etemadi, and M. Safaei, "Microbial levan biopolymer production and its use for the synthesis of an antibacterial iron (II, III) oxide–levan nanocomposite," *Journal of Applied Polymer Science*, vol. 134, no. 12, Article ID 44613, 2017.

[12] I. Khan, K. Saeed, and I. Khan, "Nanoparticles: properties, applications and toxicities," *Arabian Journal of Chemistry*, vol. 12, no. 7, pp. 908–931, 2019.

[13] M. Safaei, M. Taran, M. M. Imani et al., "Application of Taguchi method in the optimization of synthesis of cellulose-MgO bionanocomposite as antibacterial agent," *Polish Journal of Chemical Technology*, vol. 21, no. 4, pp. 116–122, 2019.

[14] M. Safaei, M. Taran, L. Jamshidy et al., "Optimum synthesis of polyhydroxybutyrate-Co_3O_4 bionanocomposite with the highest antibacterial activity against multidrug resistant bacteria," *International Journal of Biological Macromolecules*, vol. 158, pp. 477–485, 2020.

[15] M. Khan, M. R. Shaik, S. T. Khan et al., "Enhanced antimicrobial activity of biofunctionalized zirconia nanoparticles," *ACS Omega*, vol. 5, no. 4, pp. 1987–1996, 2020.

[16] H. Moradpoor, M. Safaei, H. R. Mozaffari et al., "An overview of recent progress in dental applications of zinc oxide nanoparticles," *RSC Advances*, vol. 11, no. 34, pp. 21189–21206, 2021.

[17] A. P. Ayanwale, A. d. J. Ruíz-Baltazar, L. Espinoza-Cristóbal, and S. Y. Reyes-López, "Bactericidal activity study of ZrO_2-Ag_2O nanoparticles," *Dose-Response*, vol. 18, no. 3, p. 155932582094137, Article ID 1559325820941374, 2020.

[18] S. Anandhi, M. Leo Edward, and V. Jaisankar, "Synthesis, characterization and antimicrobial activity of polyindole/ZrO_2 nanocomposites," *Materials Today Proceedings*, vol. 40, pp. S93–S101, 2021.

[19] S. L. Jangra, K. Stalin, N. Dilbaghi et al., "Antimicrobial activity of zirconia (ZrO_2) nanoparticles and zirconium complexes," *Journal of Nanoscience and Nanotechnology*, vol. 12, no. 9, pp. 7105–7112, 2012.

[20] V. Urtuvia, N. Maturana, F. Acevedo, C. Peña, and A. Díaz-Barrera, "Bacterial alginate production: an overview of its biosynthesis and potential industrial production," *World Journal of Microbiology and Biotechnology*, vol. 33, no. 11, p. 198, 2017.

[21] M. Xing, Q. Cao, Y. Wang et al., "Advances in research on the bioactivity of alginate oligosaccharides," *Marine Drugs*, vol. 18, no. 3, p. 144, 2020.

[22] L. V. Trandafilović, D. K. Božanić, S. Dimitrijević-Branković, A. S. Luyt, and V. Djoković, "Fabrication and antibacterial properties of ZnO–alginate nanocomposites," *Carbohydrate Polymers*, vol. 88, no. 1, pp. 263–269, 2012.

[23] M. Safaei and A. Moghadam, "Optimization of the synthesis of novel alginate-manganese oxide bionanocomposite by Taguchi design as antimicrobial dental impression material," *Materials Today Communications*, vol. 31, p. 103698, Article ID 103698, 2022.

[24] S.-H. Lee, "Antimicrobial effects of herbal extracts on Streptococcus mutans and normal oral streptococci," *Journal of Microbiology*, vol. 51, no. 4, pp. 484–489, 2013.

[25] G. Zhang, M. Lu, R. Liu et al., "Inhibition of streptococcus mutans biofilm formation and virulence by lactobacillus plantarum K41 isolated from traditional sichuan pickles," *Frontiers in Microbiology*, vol. 11, p. 774, 2020.

[26] A. Precious Ayanwale and S. Y. Reyes-López, "ZrO_2–ZnO nanoparticles as antibacterial agents," *ACS Omega*, vol. 4, no. 21, pp. 19216–19224, 2019.

[27] R. A. Abdulrazaq, Z. A. Al-Ramadhan, and H. H. Khalaf, "Antibacterial activity of (PVP-ZrO2) nanocomposite against pathogenic bacteria," *World News of Natural Sciences*, vol. 18, no. 2, pp. 187–194, 2018.

[28] M. Kumaresan, K. Vijai Anand, K. Govindaraju, S. Tamilselvan, and V. Ganesh Kumar, "Seaweed Sargassum wightii mediated preparation of zirconia (ZrO_2) nanoparticles and their antibacterial activity against gram positive and gram negative bacteria," *Microbial Pathogenesis*, vol. 124, pp. 311–315, 2018.

[29] R. Mekala, B. Deepa, and V. Rajendran, "Influence of dysprosium doping on structural, morphological properties and antibacterial activity of zirconia nanoparticles synthesized via Co-precipitation process," *International Journal of Nano and Biomaterials*, vol. 7, pp. 1–7, 2017.

[30] C. Sartori, D. S. Finch, B. Ralph, and K. Gilding, "Determination of the cation content of alginate thin films by FTir. spectroscopy," *Polymer*, vol. 38, no. 1, pp. 43–51, 1997.

[31] J. B. Fathima, A. Pugazhendhi, and R. Venis, "Synthesis and characterization of ZrO_2 nanoparticles-antimicrobial activity and their prospective role in dental care," *Microbial Pathogenesis*, vol. 110, pp. 245–251, 2017.

[32] J. Ayarza, Y. Coello, and J. Nakamatsu, "SEM–EDS study of ionically cross-linked alginate and alginic acid bead formation," *International Journal of Polymer Analysis and Characterization*, vol. 22, no. 1, pp. 1–10, 2017.

[33] O. Mangla and S. Roy, "Monoclinic zirconium oxide nanostructures having tunable band gap synthesized under extremely non-equilibrium plasma conditions," *Proceedings*, vol. 3, no. 10, 2019.